Supporting Information

Salio et al. 10.1073/pnas.1310050110

SI Experimental Procedures

RNA Extraction and Quantitative PCR. RNA was extracted from 10^6 cells with RNAeasy columns (Qiagen) and quantified with a Nanodrop Spectrophotometer. cDNA was synthesized from 200 ng RNA using the High-Capacity cDNA Archive kit (Applied Biosystems). Real-time quantitative PCR was performed in duplicate on the Applied Biosystems 7500 Fast Real-Time PCR system, according to the manufacturer's instructions, using Applied Biosystems Taqman Universal PCR Master mix and Taqman probes. Analysis of gene expression was calculated according to the $2^{-\Delta Ct}$ method using *GAPDH* as a housekeeping gene.

Confocal Microscopy. THP-1 cells expressing WT-CD1d (CD1d-WT) or tail-deleted CD1d (TD-CD1d) were seeded on polylysine-coated glass slides for 30 min in complete medium. The samples were fixed with 4% PFA for 15 min at room temperature and then blocked for 2 h with blocking buffer containing 10% FCS, 10% human serum, and 1% BSA, before staining with anti-human CD1d (clone 51-1-3) and anti-Lamp1 (BioLegend, cat. 328602) or anti-EEA1 (BD cat. 610456). Samples were washed three times with PBS and stained with the relevant secondary antibodies in blocking buffer for 1 h at room temperature: anti-mouse IgG1-Alexa 647 (Invitrogen cat. A21240) and anti-mouse IgG2b-Alexa 488 (Invitrogen cat. A21141). After extensive washing, glass slides were mounted (SouthernBiotech cat. 0100–20) and imaged. Confocal images were acquired using the Zeiss LSM 510 META, processed with ImageJ[88].

SI Text

Sequence of the Soluble Invariant Natural Killer T Cell T-Cell Receptor-β Chain Used in This Study. (Nomenclature accordingly to the International Immunogenetics database)

Vβ11 sequence: CASS
N-Dβ-N: PALAGP
Jβ2.1 sequence: SYNEQFFGPGTRLTVL

Model Description. The molecules we include in the model are saposin (S), a population of irrelevant lipids (L), a population of relevant lipids (L*), and CD1d bound to irrelevant and relevant lipids (C and C*, respectively). A simplified schematic showing the interactions between these molecules is shown in Fig. 4*A*.

We assume that in the absence of Saposin there is a background exchange of lipids,

$$C + L^* \overset{b_{cat}}{\leftrightarrow} C^* + L,$$

where b_{cat} is the rate constant (in units of $\mu M^{-1}\cdot s^{-1}$) of background saposin-independent lipid exchange, which we take to be equal for both the relevant and irrelevant lipid. We allow saposin to directly bind both relevant and irrelevant lipids,

$$S + L^* \overset{sk_{on},sk_{off}}{\leftrightarrow} SL^*$$

$$S + L \overset{sk_{on},sk_{off}}{\leftrightarrow} SL,$$

where SL* and SL are the saposin bound to the relevant and irrelevant lipid, respectively, and k_{on} and k_{off} are the on-rate (in units of $\mu M^{-1}\cdot s^{-1}$) and off-rate (in units of s^{-1}), respectively. When bound to lipids, saposin is able to bind to CD1d and exchange lipids,

$$C + SL^* \overset{ck_{on},ck_{off}}{\leftrightarrow} CSL^*$$

$$CSL^* \overset{ck_{cat}}{\rightarrow} C^* + SL,$$

where CSL* is a complex formed between CD1d (with irrelevant lipid) and saposin carrying a relevant lipid. This intermediate complex can either dissociate without catalysis (ck_{off} in units of s^{-1}) or exchange lipids and dissociate (ck_{cat} in units of s^{-1}). This lipid exchange is modeled as a classic enzymatic reaction. Note that the identical reaction is also possible with the irrelevant lipid,

$$C^* + SL \overset{ck_{on},ck_{off}}{\leftrightarrow} C^*SL$$

$$C^*SL \overset{ck_{cat}}{\rightarrow} C + SL^*,$$

where C*SL is a complex formed between CD1d (with relevant lipid) and saposin carrying an irrelevant lipid.

We have included an interaction between CD1d and saposin despite the fact that we have not observed such a complex in our surface plasmon resonance (SPR) experiments. We expect such a complex to form given that saposin does increase the exchange rate of lipids with CD1d.

We emphasize that in this mathematical model, neither CD1d nor saposin can differentiate between the relevant and irrelevant lipids, which can be seen by the fact that all reaction rates involving the relevant lipid are identical to those involving the irrelevant lipid.

Parameter Values. The reaction rate constants used for the model are shown in Table S2. In addition, the concentration of CD1d was taken to be 10 μM and the concentration of the irrelevant lipid was taken to be 1,000 μM. The concentration of saposin and the relevant lipid were varied.

The precise rate of lipid exchange in the presence or absence of saposin is presently unknown. We have therefore assumed a low rate of exchange in the absence of Saposin (small b_{cat}) and a large rate of exchange in the presence of Saposin; it follows that the timescales shown in Fig. 4*D* are approximations, but we emphasize that the key observation is that saposin decreases the timescale of lipid exchange.

Model Calculations. The system of ordinary differential equations corresponding to the reactions described above were generated in BioNetGen and integrated in Matlab (Mathworks) (1).

1. Faeder JR, Blinov ML, Hlavacek WS (2009) Rule-based modeling of biochemical systems with BioNetGen. *Methods Mol Biol* 500:113–167.

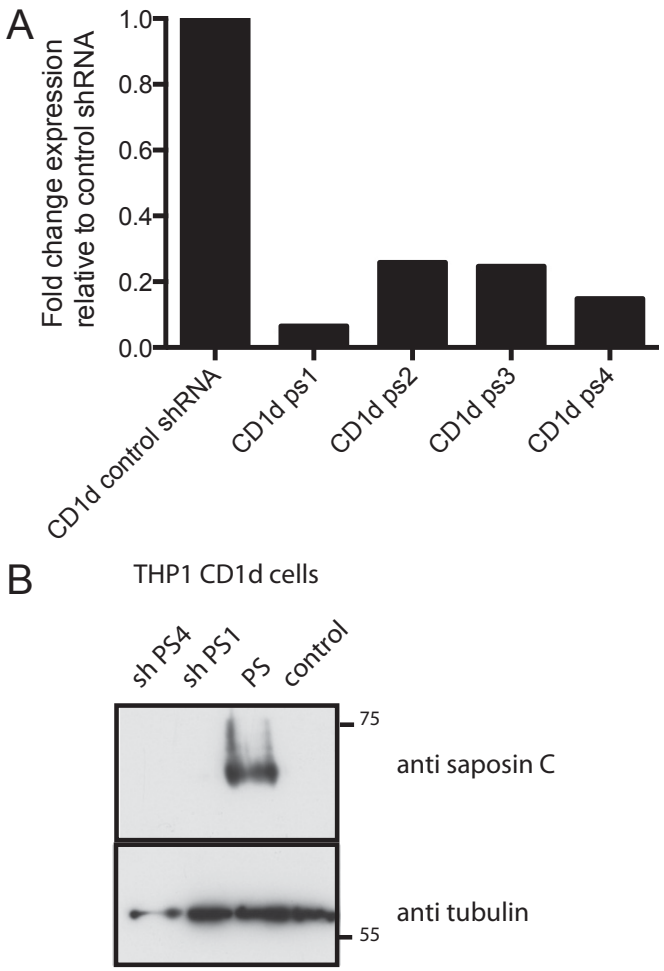

Fig. S1. Generation of prosaposin deficient THP-1–CD1d cells. (*A*) THP-1–CD1d cells were transduced with either control shRNA or four different prosaposin shRNA lentiviruses (Sigma; Mission shRNA). Knockdown was validated by quantitative PCR (Taqman Probes, Applied Biosystems) and fold-change expression of prosaposin relative to control shRNA was calculated according to the $2^{-\Delta Ct}$ method. (*B*) Lysates from THP-1–CD1d cells transduced with control shRNA (control), prosaposin shRNAs (shPS1, shPS4), or overexpressing prosaposin (PS) were blotted with antisaposin C antibody and antitubulin. Because of sensitivity issues, we were unable to detect endogenous expression of prosaposin protein by Western blot, which was only detectable in the lysate of cells in which prosaposin was overexpressed (PS).

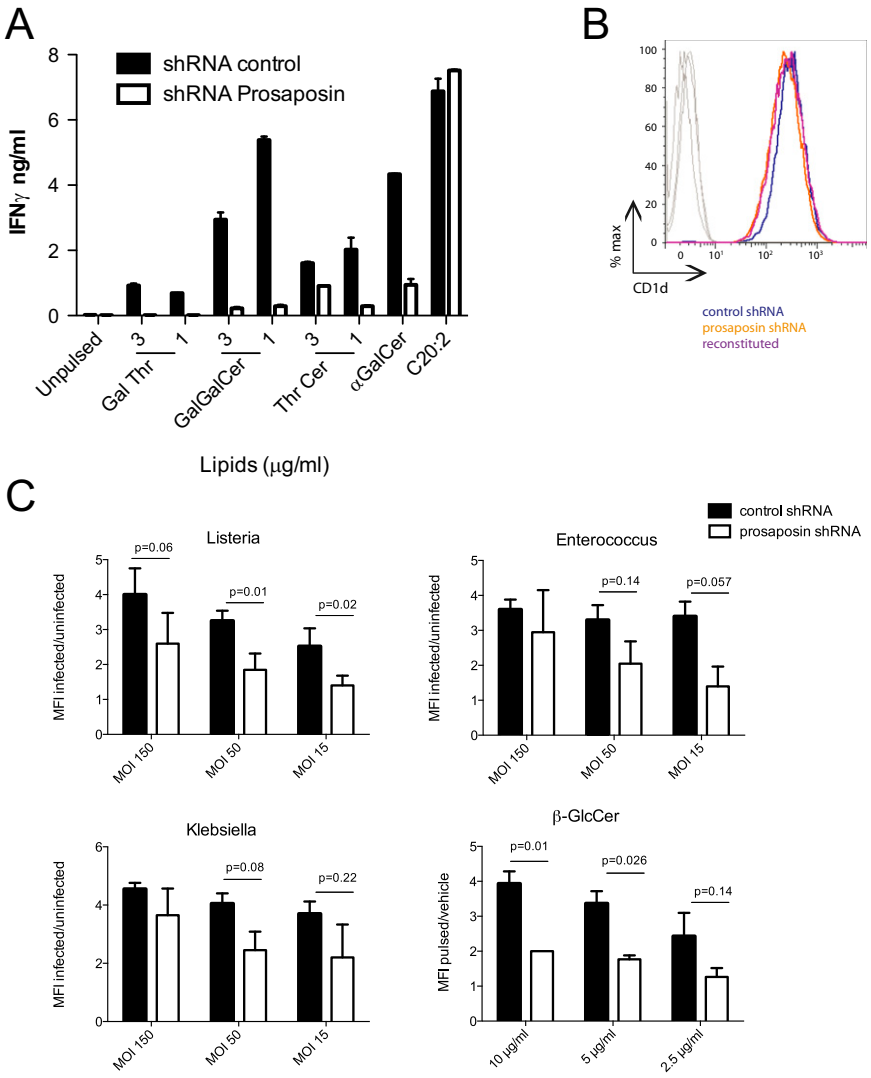

Fig. S2. Presentation of CD1d-binding synthetic and self lipids is saposin dependent. (*A*) THP-1–CD1d cells transduced with control or prosaposin shRNA were pulsed with the indicated lipids [3 μg/mL and 1 μg/mL, except α-galactosyl ceramide (α-GalCer) 200 ng/mL and C20:2 100 ng/mL] and incubated with invariant natural killer T (iNKT) cells. IFN-γ secreted in the supernatant at 36 h was measured by ELISA. Data are representative of three independent experiments (mean ± SD). (*B*) CD1d surface expression of the cells shown in Fig. 1. Gray lines represent isotype control stained cells. (*C*) THP-1–CD1d cells transduced with control or prosaposin shRNA were infected with *Listeria monocytogenes*, *Enterococcus faecalis*, or *Klebsiella aerogenes*, at the indicated multiplicity of infection (MOI) or pulsed with β-GlcCer at the indicated concentrations. Cells were stained with soluble iNKT T-cell receptor (TCR) tetramers and the average mean fluorescence intensity ratio of infected/uninfected cells or pulsed/unpulsed cells is shown. Data are pooled from four (*Listeria*) or three independent experiments.

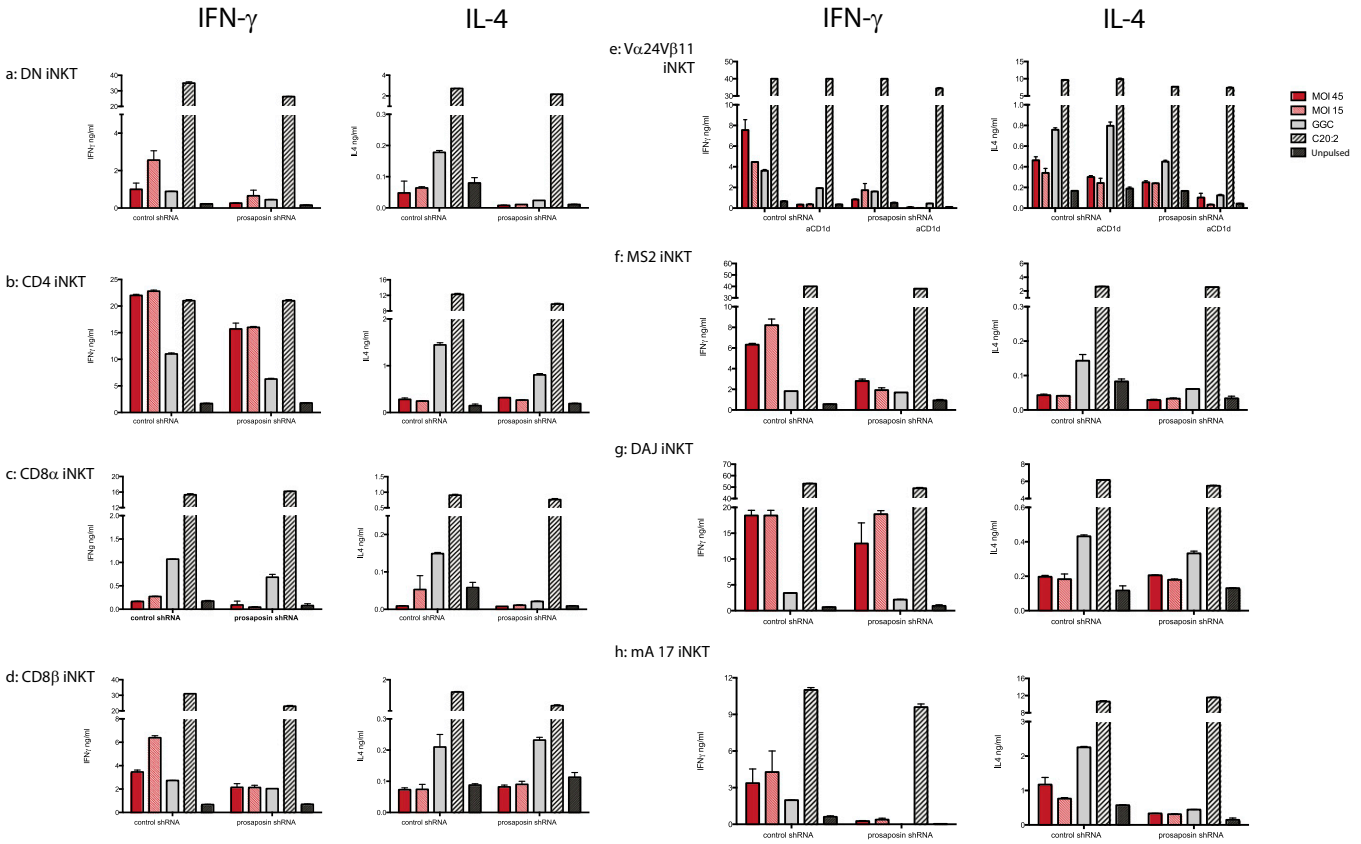

Fig. S3. Presentation of CD1d-binding self lipids is saposin dependent. THP-1–CD1d cells transduced with control or prosaposin shRNA were infected with *L. monocytogenes* at the indicated MOI or pulsed with glycolipid Gal(α1→2)GalCer (GalGalCer; GGC, 5 ng/mL) or C20:2 (20 ng/mL) and incubated with eight different iNKT cell lines (phenotype described in the Table S1). Line Vα24Vβ11 was also tested in the presence or absence of the anti-CD1d blocking antibody (the same data for line Vα24Vβ11 are also shown in Fig. 1*B*). IFN-γ and IL-4 secreted in the supernatant at 36 h were measured by ELISA (mean ± SD).

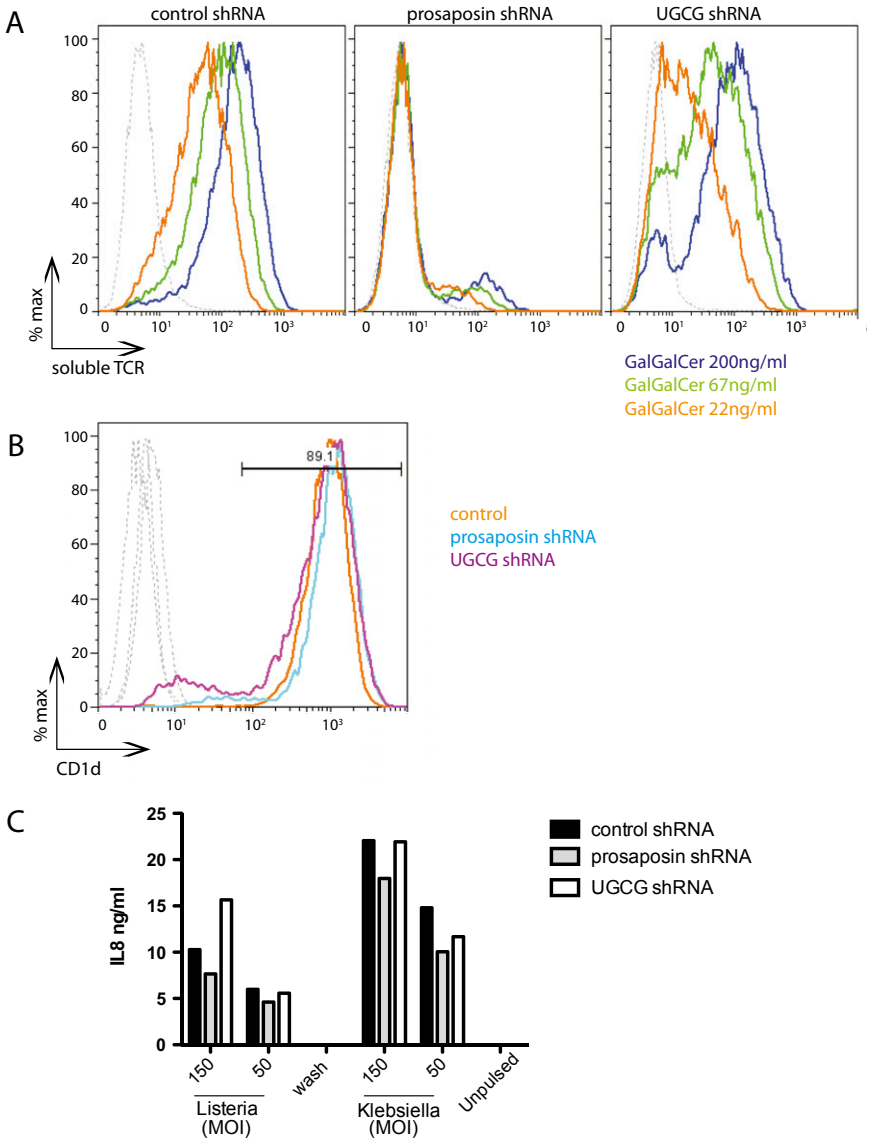

Fig. S4. (*A*) THP-1–CD1d cells transduced with control (*Left*), prosaposin (*Center*), or β-glucosylceramide synthase (*UGCG*) shRNA (*Right*) were pulsed overnight with the indicated concentrations of GalGalCer. Flow cytometry of cells stained with soluble iNKT TCR tetramers is shown. Data are representative of five independent experiments. Gray dotted lines represent vehicle pulsed cells. (*B*) CD1d surface expression of the cells shown in *A*. The apparently lower GalGalCer presentation by *UGCG* THP-1 cells is accounted for by a lower percentage of cells expressing high levels of CD1d. However, cells used for the experiment shown in Fig. 1*B* had been sorted to equalize CD1d expression. (*C*) IL-8 secretion by THP-1–CD1d cells transduced with control, prosaposin or *UGCG* shRNA and infected with *L. monocytogenes* or *K. aerogenes* at the indicated MOI. Wash: supernatant from the bacterial growth.

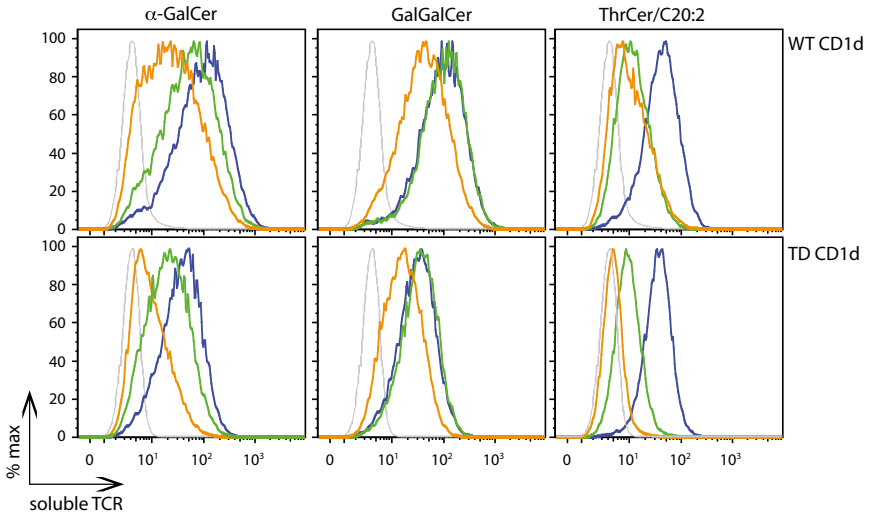

Fig. S5. Staining with soluble iNKT TCR tetramers of THP-1–expressing WT or TD-CD1d molecules upon pulsing with α-GalCer (*Left*; 300, 100, 30 ng/mL), GalGalCer (*Center*; 600, 200, 70 ng/mL), ThrCer (*Right*, orange; 200 ng/mL), and C20:2 (*Right*, blue and green; 150, 50 ng/mL). Gray dotted lines: vehicle pulsed cells. Data are representative of three independent experiments.

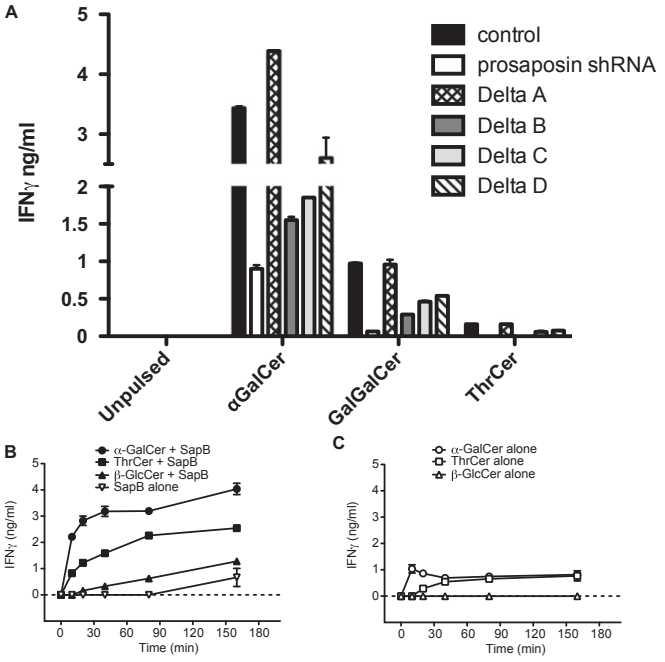

Fig. S6. (*A*) THP-1 cells transduced with control, prosaposin shRNA, or the latter transduced with constructs encoding for mutant prosaposin molecules, each lacking an individual saposin [Delta A, B, C or D; see Yuan et al. (1)] were pulsed with α-GalCer (50 ng/mL), GalGalCer (100 ng/mL), or ThrCer (20 ng/mL) and incubated with iNKT cells. IFN-γ secreted in the supernatant at 36 h was measured by ELISA (mean ± S.D.). Data are representative of three independent experiments. (*B* and *C*) Human CD1d molecules immobilized on streptavidin plates were loaded for the indicated time with 1 μg of each lipid with (*B*) or without (*C*) 50 μg/mL of saposin B. iNKT cells were added and IFN-γ secreted in the supernatant at 36 h was measured by ELISA. Data are representative of five independent experiments (mean ± SD). Note that saposin B purified from *Escherichia coli* carries an antigenic bacterial lipid that can be loaded on CD1d molecules after 2.5 h. Consistent with this observation the crystal structure of saposin B dimer (2) revealed the presence of phosphatidylethanolamine (PE).

1. Yuan W, et al. (2007) Saposin B is the dominant saposin that facilitates lipid binding to human CD1d molecules. *Proc Natl Acad Sci USA* 104(13):5551–5556.
2. Ahn VE, Faull KF, Whitelegge JP, Fluharty AL, Privé GG (2003) Crystal structure of saposin B reveals a dimeric shell for lipid binding. *Proc Natl Acad Sci USA* 100(1):38–43.

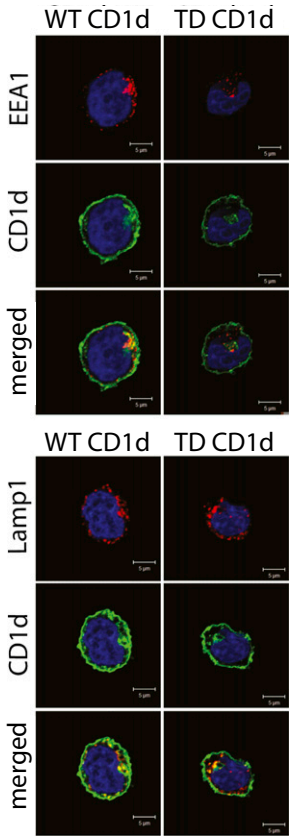

Fig. S7. Endolysosomal distribution of WT and tail-deleted CD1d molecules. Confocal microscopy of THP-1 cells expressing WT or tail-deleted CD1d molecules (TD-CD1d) molecules. Cells were stained with anti-human CD1d (green) and anti-Lamp1 or anti-EEA1 antibodies (red); nuclei were visualized with DAPI. Shown are representative confocal images obtained using a Zeiss LSM 510 META (Scale bars, 5 μm.)

Table S1. Phenotype of the iNKT cell lines used in this report

Cell lines	Phenotype	CD161
Vα24Vβ11	50% CD8α; 36% DN; 11% CD4	6%
MS2	32% CD8α; 59% DN; 8% CD4	72%
mA17	9% CD8α; 30% DN, 60% CD4	43%
DAJ	47% CD8α; 48% DN, 4% CD4	90%
CD8α	$CD8\alpha^+$	80%
CD8β	$CD8\alpha^+\beta^+$	10%
CD4	10% CD8α; 90% CD4	10%
DN	36% CD8α; 64% DN	100%

Eight NKT lines were used in this study and the phenotype is indicated in the table. The lines were all α-GalCer–CD1d tetramer$^+$ $V\alpha24^+V\beta11^+$. The lines were derived either by direct antibody sorting from peripheral blood mononuclear cells (Vα24Vβ11) or after priming with dendritic cells pulsed with α-GalCer as described in Gadola et al. (1). Cells were stained with a combination of α-GalCer–CD1d tetramer, Vα24 (Immunotech), Vβ11 (Immunotech), CD4 (BD Pharmingen), CD8α (BD Pharmingen), and CD8β and CD161 (eBiosciences) antibodies.

1. Gadola SD, Dulphy N, Salio M, Cerundolo V (2002) Valpha24-JalphaQ-independent, CD1d-restricted recognition of alpha-galactosylceramide by human CD4(+) and CD8alphabeta(+) T lymphocytes. *J Immunol* 168(11):5514–5520.

Table S2. Parameter values

Parameter	Value	Units
b_{cat}	10^{-6}	$\mu M^{-1}\cdot s^{-1}$
sk_{on}	1.0	$\mu M^{-1}\cdot s^{-1}$
sk_{off}	0.01	s^{-1}
ck_{on}	1.0	$\mu M^{-1}\cdot s^{-1}$
ck_{off}	10	s^{-1}
ck_{cat}	1.0	s^{-1}